Tines/No-Tines Trade-off Study for MSL Coring

Daniel Helmick
Paul Backes

May, 2005

1. Introduction

The MSL mission will have a rover with a manipulator arm that caries a coring tool. This coring tool may or may not have tines. Tines are rigid structures that contact the surface to increase the stiffness between the coring bit and the environment. They would be similar in concept to the 'butterfly wings' on the MER RAT. In this document we discuss the advantages and disadvantages of using the tines and no-tines methods for coring from a robotic arm and we document an extensive amount of experimentation that was performed to compare these two techniques. In Section 2, requirements for the coring process are discussed. In Section 3, arm design assumptions that were made for this comparison are listed. In Section 4, the two different coring methods compared in this document, tines and no-tines, are described in detail. In Section 5, the criteria that are significant to the tines/no-tines comparison are discussed in detail. In Section 6, the experimental setup is detailed. In Section 7, the experimental results are shown. Section 8 is a summary of this discussion.

2. Coring Requirements

Requirements for the coring process were taken from [1]. A summary of these requirements that impact the tines/no-tines discussion follows:

- Operate over angles from vertical down to horizontal to 45° up (0 to 135° with 0° being the corer pointing vertically down)
- Size of core – 0.8 to 1.2 cm diameter; 10 to 12 cm length
- Coring rate – 5 cm/hr
- Average axial preload force (RMS over any 0.1 s) less than 80 N
- Maximum lateral force (e.g. when starting hole) less than 15 N
- Ability to take intact cores

3. Arm Design Assumptions

Figure 1 shows the current baseline design of the arm. The configuration of the arm is described below.

3.1. Degrees of Freedom

It is assumed that the arm will have five degrees of freedom (DOFs) with a joint configuration of yaw, pitch, pitch, pitch, yaw (YPPPY). This is the same configuration as MER.

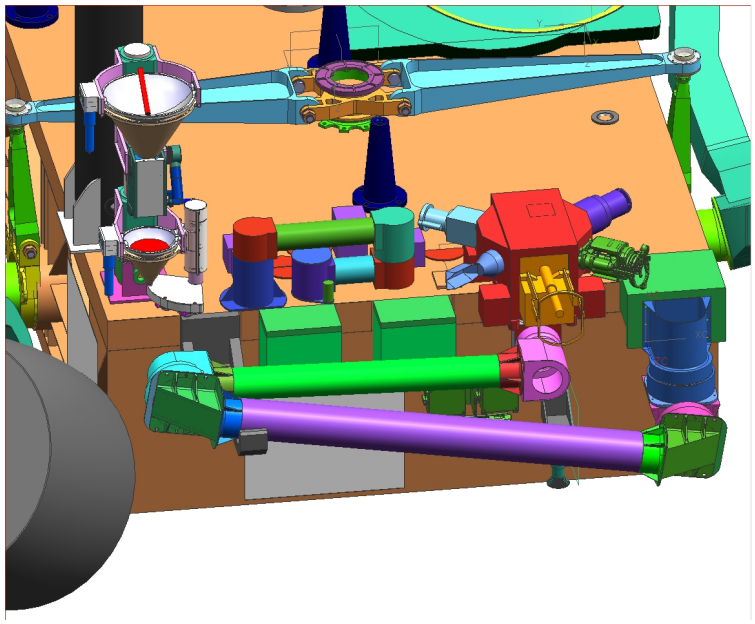

Figure 1: Baseline MSL Arm Design

3.2. Links

The baseline arm design uses link lengths of at least 0.75 meters, making the overall arm length at least 1.5 meters (and potentially up to 2 meters). This is at least twice the length of the IDD on MER.

3.3. Actuator Design

Joint design parameters were taken from [2] and are summarized as follows:

- Brushless motors (see Figure 2) – early motor torque constant values are ~15 in-oz/amp
- Titanium planetary gear train
- Harmonic drives to output shafts
- Electro-magnetic brake – uses discrete mechanical detents (see Figure 2)
- Position sensing (hall effect sensors and relative encoders on motors, and resolvers/absolute encoders on output shafts)
- Bus commanded (read/command cycle frequency for 5 motors on bus ~10Hz)
- Motor control loop at ~2kHz

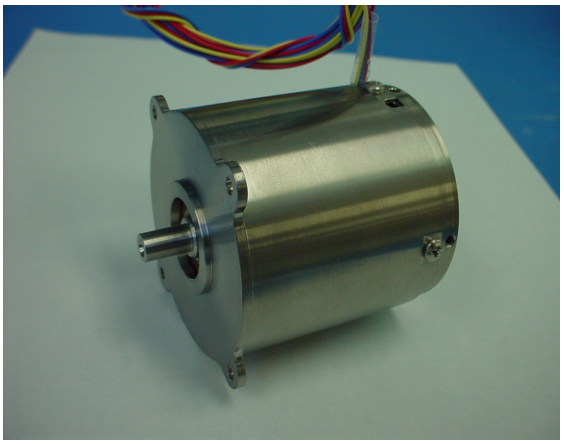


Figure 2: MSL Brushless Motor (left) and Electro-magnetic Brake (right)

4. Coring Options

This section describes the two approaches to coring that are compared in this report.

4.1. Tines

This section describes the tines approach to coring. It describes the motivation and background behind the tines approach. The fundamental concept of the tines approach is to increase the stiffness between the coring tool and the environment by creating a rigid contact to the environment close to where the tool will be coring. A more detailed description of the tines approach actually used in experimentation is described in Section 6.

4.1.1 Background – MER RAT

Due to the similarities between ratting and coring, the RAT design (see Figure 3) and operation is summarized here. This design is the motivation for the tines concept of coring.

Here is a summary of the MER RAT tool [3,4,5]:

- Operation: Move to surface until contact switches sense contact; overdrive arm to a setpoint within the rock to apply the preload; setpoint is computed using the arm stiffness model
- Maximum preload used was 70N commanded; actual preload was significantly less than commanded; at 60N commanded preload the actual preload was 40N +/- 10N
- Contact switches integrated with the butterfly mechanism
- Joints have detents that prevent backdriving during ratting; arm does not servo during ratting
- Original design of butterfly wings used spikes to ensure rigid contact; but rigid contact was found to be a problem in that it caused torque buildup due to rotational motion around tool axis during preload (due to link flexibility); with rough surface balls on butterfly wings in final design, it enables some slippage of contact points during preload

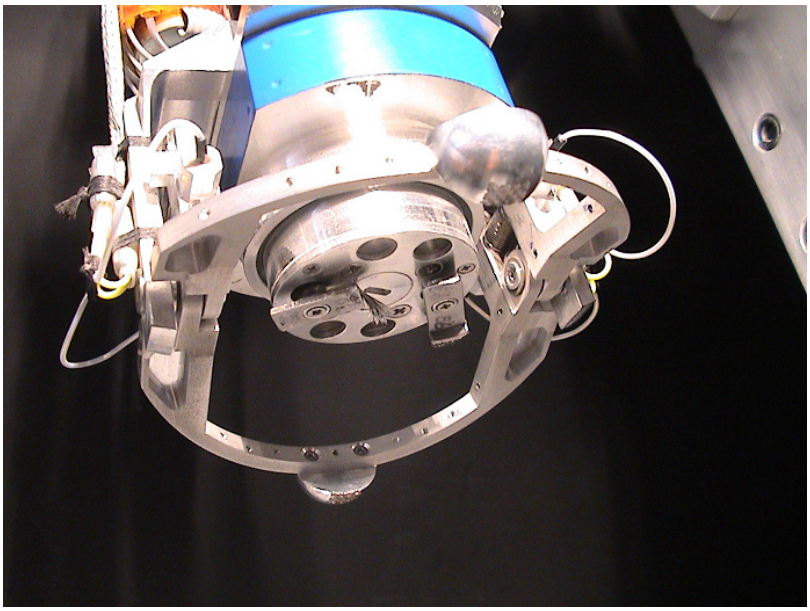

Figure 3: MER RAT with Butterfly Wings

4.1.2 MSL Tines Configuration

Although the functionality of the RAT butterfly wings is similar to the requirements of the MSL tines there are fundamental differences. The most consequential difference is the fact that if the tines slip while coring, a catastrophic failure of the coring tool could occur. If the butterfly wings slip while ratting, the tool simply stalls. This difference is due to the fact that while coring down to 10cm, the tool and the environment are much more tightly coupled than when ratting to 5mm. This difference will most likely lead to a significantly different design for the tines.

The tines configuration for the Honeybee corer to be used on the MSL Brassboard SA/SPaH (Sample Acquisition/Sample Processing and Handling) system is shown in Figure 4. It is nearly identical in design to the RAT butterfly wings. The tines used in the coring experiments described in this document are shown in Figure 12.

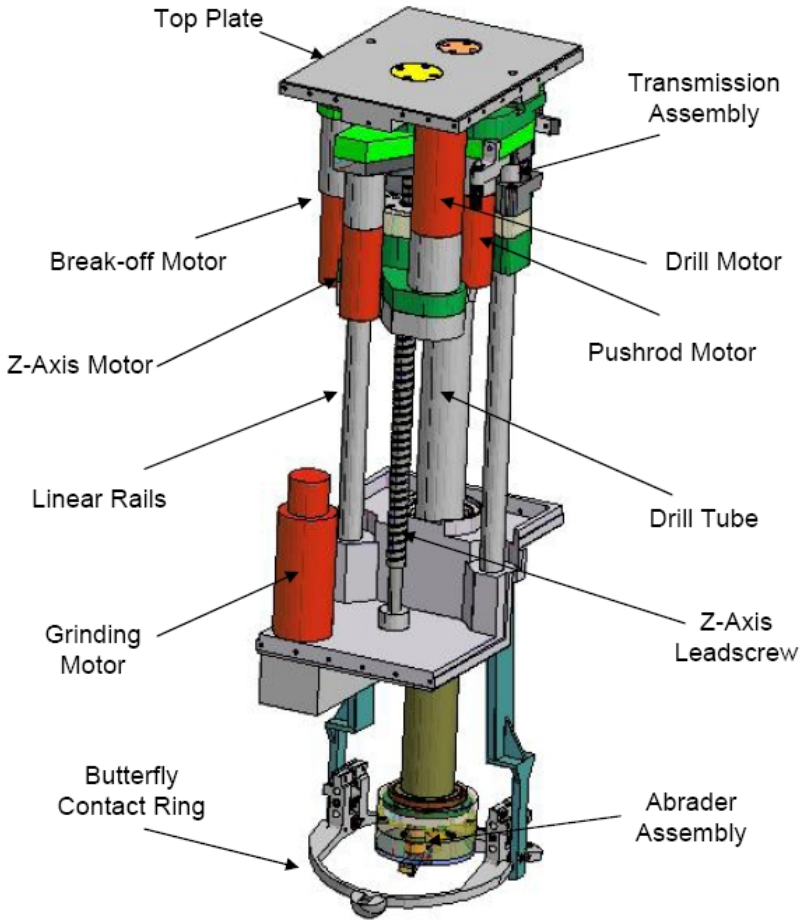

Figure 4: Current Honeybee Corer/Abrader Design

4.1.3 Tines Coring Algorithm

The nominal algorithm for tines coring is described in this section. A more detail description of the actual algorithm used in experiments is described in Section 6.2.3. Manual target selection would occur in mast or hazard camera imagery. Target position and normal would be calculated from stereo imagery. The algorithm to determine the target normal in the tines case would most likely be slightly different than is typically used. With three tines separated by significant distances, the 'tines normal' would most likely be calculated using a kinematic model of the tines centered on the target. This is opposed to the typical surface normal calculation done by MER and could result in significantly different estimates depending on the topology of the rock. Once the target position and normal were calculated, the arm would be commanded to go to a pose close to the target position and normal. At this step, the preload step, two approaches could be taken. The first approach would be to use the MER algorithm (move until touch; use flexibility model to calculate correct overdrive for desired preload). The second approach would be to measure the preload force using motor currents, joint torque sensors, link strain gages, or a wrist force/torque sensor (all of these approaches are compared in [6]). The second approach would result in more accurate preload magnitude and direction. The magnitude of the preload applied

would need to be larger than the largest expected coring forces (including percussive spikes if using a percussive coring method) plus margin, in order to prevent the tines from walking during the coring process. After a preload was applied, the coring process would then begin. Several different methods for coring could be taken. The first involves open loop feed rate control. This would simply be the selection of a feed rate that was slow enough to core through the hardest rock expected. This approach would not be effective when the range of the strength of the rocks to be cored is wide, because, as will be shown later, coring rate is a strong function of rock compressive strength. The second method would be to use a model-based feed-forward open loop control that would estimate the desired feed rate based on likely rock properties. However, it is difficult to accurately estimate the rock mechanical properties with non-contact instruments. The third method would be to vary the feed rate based on the current feedback of either the rotary motor or the linear stage motor. The fourth method would be to add a single axis force sensor between the linear stage and the corer and vary the feed rate based on the force feedback. Comparison of these different techniques is beyond the scope of this document.

4.2. No-tines

The concept of no-tines coring is to not use any tines to increase the stiffness between the tool and the environment. There are two fundamental differences between tines coring and no-tines coring. The first difference is how the linear motion required for coring is provided. In tines coring, this linear motion is provided by a linear stage between the tines and the coring bit. In no-tines coring, a Cartesian motion enabled by the 5 DOFs of the arm provides the linear motion. The second difference is the fact that force sensing on the arm [6] can be used to observe the coring process, as opposed to the tines approach where any sensors used to observe the coring process must be between the tines and the coring tool. A more detailed description of the no-tines approach actually used in experimentation is described in Section 6.

4.2.1 No-Tines Coring Algorithm

Target position and normal vector would be calculated in the same manner as MER, using mast or hazard camera imagery. The arm would be commanded to go to a pose close to the target position and normal. Several approaches could be taken for no-tines coring. Most are very similar to those of the tines coring method described above, and have the same advantages and disadvantages. The first approach would be to use open loop feed rate control and select a feed rate that was slow enough to core through the hardest rock expected. The second approach would be to use a model-based feed-forward open loop control that would estimate the desired feed rate based on likely rock properties. The third approach would be to vary the feed rate based on the current feedback of the rotary motor of the coring tool. The fourth approach would be to vary the feed rate based on one of the force sensing methods described in [6]. The fifth approach would be to vary the feed rate and the 4 other controllable DOFs of the arm in order to minimize the binding forces of coring. The last approach is the only approach that is not possible using the tines technique. Discussion of the force control algorithms used in these different techniques is beyond the scope of this document. A detailed discussion of the technique actually used in experimentation is described in Section 6.2.2.

5. Tines/No-tines Comparison Criteria

5.1. Stiffness of Tool Relative to Environment

The differences between the tines and the no-tines coring techniques are most substantial for the category of stiffness of the tool relative to the environment. Nowhere else are the two techniques so disparate. By directly interacting with the environment close to the coring location, the tines are inherently able to create much higher stiffness than the no-tines approach.

As can be seen in Section 7, the stiffness of the tool relative to the environment does not seem to affect the ability to take an intact core. Using both methods we have been able to achieve intact cores in our experiments. There are several other criteria it does affect however. Conceivably, if the tool/environment stiffness were high enough, then it would be possible to start the coring process without a centering bit. The kind of stiffness required for this functionality would, for all practical purposes, demand the tines technique. It does not seem feasible (with the considerable knowledge gained from experimentation) to create an arm stiff enough (of the length needed for MSL) to core without a centering bit without using special techniques, such as starting a core with percussion and no rotation, to avoid walking of the bit. It is beyond the scope of this document to discuss these special techniques.

A negative aspect to having the high tool/environment stiffness that is created by the tines is that small motions between the tool and the environment create high, potentially dangerous, forces. These high forces may result in several undesirable outcomes: slippage of the tines (Section 5.3), binding of the tool (Section 5.4), or tool damage.

5.2. Tool Alignment with Surface Normal

The surface normal defined by the tines contact points with the environment may be significantly different from the surface normal where the tool interacts with the environment. This fact could potential create large side loads on the bit when starting the coring process. This problem could be solved operationally by only selecting targets with large (relative to the tines spacing) flat areas, but this could severely limit target selection.

For no-tines coring, the tool alignment error would come entirely from surface normal measurement error and arm kinematic errors. This issue places no constraints on target selection for no-tines coring.

5.3. Tine Slip

For coring with tines, a serious failure mode is slippage of the tines on the surface. It is serious because the tines may be resisting significant forces with the environment. If the tines slip, then those forces would be transferred to the tool most likely causing the tool to fail.

5.4. Tool Binding

5.4.1 Detection

With tines, detection of binding could be done with the use of a model of rotation rate, feed rate, and motor current of tool to detect binding. Another technique to detect binding with the tines method would be to use a lateral (2 DOF) force sensor between the tines and the tool. Without this type of a sensor, binding forces could not be measured. Any sensing on the arm would be isolated from the coring process by the tines, making the binding forces unobservable.

With the no-tines approach, it is possible to measure interaction forces between tool and environment using force sensing on the arm [6]. It would also be possible to detect binding using the same model based technique described in the above paragraph.

5.4.2 Accommodation

With the tines approach the only type of accommodation that is possible would be to stop coring, retract the coring bit, remove the preload, select a different target (this could potentially mean moving the rover), and start the coring process over again. This could potential take several sols to accomplish. The reason that a new target needs to be selected is because of the danger of coring close to a pre-existing hole. This is a risky operation due to the chance of the coring bit entering the previously cored hole. Also, attempting to core in the same hole after repositioning the arm is also a risky operation because of the required accuracy of the placement.

With the no-tines approach, an active binding accommodation algorithm could be used to minimize the lateral forces and off-tool-axis torques if one of the force sensing methods discussed in [6] was in place. This algorithm would allow for the accommodation of binding without interruption of the coring process. Discussion of the details of this algorithm is beyond the scope of this document.

5.4.3 Likelihood of Binding

In all of the tines and no-tines experimentation that we have performed, we have not experienced any binding. These results should not be construed to mean that it could not happen, but only that it is a rare event with the configurations that have been used in experimentation. A significant difference between the experiments described in this document and the flight system may be that fact that a percussive drill was used in these experiments. If a non-percussive corer is used in the flight system, an increase in the risk of binding may occur.

5.5. Normal Force

The force discussed in this section (referred to as the ‘normal force’) is the preload force for the tines approach and the coring force for the no-tines approach because these are the forces that the arm actually has to apply to the environment. The actual coring force for both methods is assumed to be equal. From experimentation the coring force is known to be a function of coring depth and rock properties. When using a percussive drill, the coring force is defined as a filtered force that does not include the impulse forces from the percussive action.

When comparing the coring force of the no-tines approach to the preload force of the tines approach, the most significant difference is the magnitude. The preload force must necessarily be significantly larger than the coring force in order to prevent walking of the tines. For example, in our experiments (see Section 7) a preload force of 130 N was used when the coring force was known to be 100-120 N. It is most likely that an even larger margin would be required for a flight system.

This higher preload results in many ramifications on the arm design and operation:

- Higher requirements for: joint torque, joint stiffness, link strength, and link stiffness
- More constraints on the rock selection; rock selection would necessarily depend on factors (such as rock mass, geometry, etc.) that would prevent the rock from moving during the coring process, and a higher force would mean less selection
- Greater risk of damaging the arm or corer if the force is released due to slippage of the tines
- Higher arm deflections and more reliance on the flexibility model of the arm which becomes more non-linear with the magnitude of the deflections

5.6. Link Stiffness

Link stiffness has several effects on the tines/no-tines decision. The main motivation for using tines is to increase the stiffness between the tool and the environment.

In the tines approach, after the preload is applied to the tines, the link stiffness would have very little effect on the tool/environment stiffness. However, during the application of the preload, the stiffness of the links would have a large effect. For less stiff links, more twist would occur while preloading. This twist could cause slippage of the tines, or unwanted internal forces between the tines. Also, the fact that the preload must be significantly higher than the coring force would most likely increase the stiffness requirements of the links.

In the no-tines approach, the link stiffness is the largest contributor to the stiffness between the tool and the environment. The no-tines stiffness requirement is unknown; however, it has been proven by experimentation that it is possible to take an intact core with a very compliant arm (see Section 7.1).

5.7. Rock Size and Geometry

The tines approach would require a larger flat surface area on the rock than no-tines approach in order to have the tines vector aligned with the target surface normal. The tines approach would also place greater constraints on the surface large-scale roughness because of a necessary maximum allowable protrusion of the rock through the tines plane, due to a potential collision between the bit and the protruding rock. This would not be a constraint on the no-tines approach.

The tines approach would also increase the preload required as discussed in Section 5.5; this, in turn, would increase the lower bound on rock size selection in order to avoid movement of the rock while coring.

5.8. Energy Consumption

It is assumed that the actual energy required for the physical act of coring will be approximately the same for the tines and the no-tines approach. The difference comes in the efficiencies of the systems used to core. In the tines approach a higher preload is applied by all five DOFs of the arm and then the brakes are applied. Then the entire energy for coring comes from the 2 DOFs required for coring (rotation and translation of the bit). In the no-tines approach all five DOFs of the arm plus the rotational DOF of the corer are used to provide the energy necessary for the coring process.

If the torque constants of all of the motors and all of the gear train efficiencies were equal then the no-tines approach would take less energy (because of the lower preload). The outcome of this comparison also depends on whether the brakes are normally-locked, normally-unlocked, or bi-stable. If the brakes are normally-locked then this benefits the tines-approach, if the brakes are normally-unlocked then this benefits the no-tines approach, if the brakes are bi-stable then this is equivalent for both cases. It is unclear (without experimental validation) which approach is more efficient.

One fact to note is that in the tines approach, unlike in the no-tines approach, most of the energy for coring would be going through the linear stage of the corer. Therefore the efficiency of the tines approach would be highly dependent upon the efficiency of the linear stage.

5.9. Mass

Three factors almost certainly increase the mass of an arm using the tines approach relative to the no-tines approach. The first factor is that the mechanical complexity of the tines approach is greater, thus requiring more material and mechanics. The extra DOF would require at least one extra motor/gear train assembly, and the tines themselves would add mass. The second factor is the fact that all of the extra mass of the tines approach needs to be added at the end of the arm which would increase the required joint torques which would increase the mass of the joints and links. The third factor is the fact that the tines approach requires a higher preload, again requiring higher torques from the joints, and thus adding mass.

5.10. Complexity

In this section we discuss the impact of the tines/no-tines approaches on the complexity of the manipulator/corer system. Complexity includes controls complexity and electro-mechanical complexity.

For the tines approach the electro-mechanical complexity is higher than the no-tines approach. An at least one extra DOF is necessary to provide the translation after preload. It is likely that additional sensing would be required due to the fact that the tines isolate the coring system from

the arm system, thus making the coring process unobservable by any sensors on the arm. Conversely, the no-tines approach allows for a simpler tool that only needs to provide rotation of the bit.

The controls complexity comparison depends on the method of coring used for no-tines coring. An algorithm very similar in complexity to the preload algorithm for the tines approach could be used for coring in the no-tines approach. In fact, a nearly identical algorithm was used in the experiments described in Section 6.2.

6. Experimental Setup

6.1. Hardware

6.1.1 Common

6.1.1.1. Joints

The joints used for both the tines and the no-tines experiments were commercial-off-the-shelf (COTS) components (Figure 5) sold by a German company, Amtec-Robotics, called Powercubes. They are entirely self-contained (with standard mechanical and electrical interfaces) and only require power and communication to control. These joints are very similar in design to those being designed for MSL (see Section 3.3), with the major difference being a factor of ~50 lower gear ratio (and thus much higher current draw per torque output). The joints were sold in three sizes of varying torque capacities (see Table 1). Figure 7 shows the capability of the joints to follow a precise trajectory under load (note that there are actually two point plots in this figure, but the trajectory is very precise, so they overlap). Below is a summary of the specifications of the joints:

- Brushless motors
- 500 count encoders
- 160:1 harmonic drives
- Microcontroller based PID position control at 4 kHz
- CANbus interface (1Mbs) – allows for synchronized/coordinated motion control at ~200 Hz for a 5 DOF arm
- Electro-magnetic brakes

Figure 5: Amtec Powercube Joint

Specification	PR110	PR90	PR70
Nominal Torque (N-m)	112	62	21
Resolution (ticks/deg)	888	888	888
Max. Velocity (deg/sec)	150	150	150
Repeatability (deg)	+/- 0.02	+/- 0.02	+/- 0.02
Power (W)	500	250	125
Mass (kg)	6.6	3.8	1.8

Table 1: Specifications for the Three Sizes of Powercube Joints Sold by Amtec-Robotics

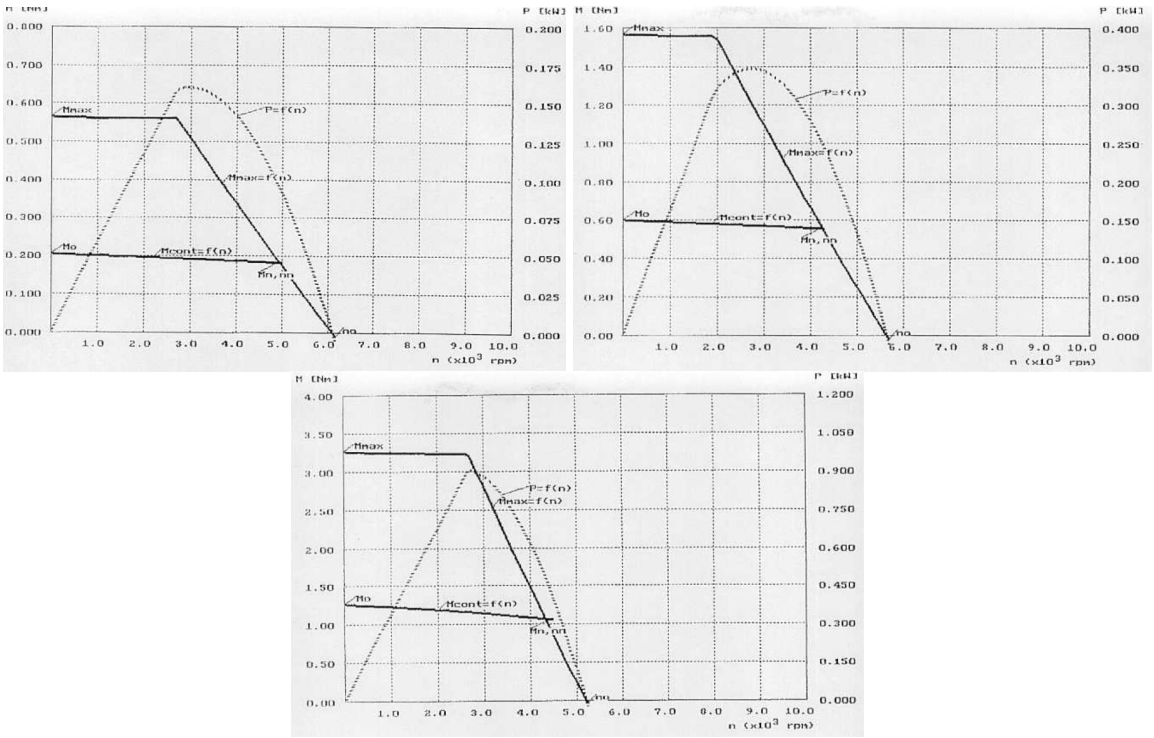

Figure 6: Torque/Power Curves for the Motors Used in the Powercube Joints

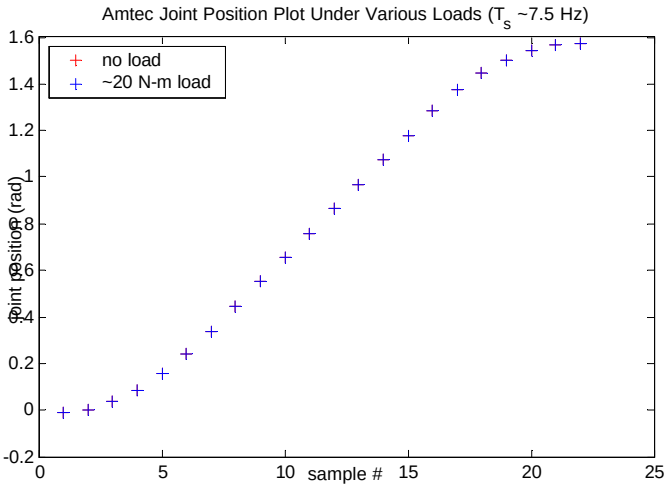

Figure 7: Position Plot of No-load vs. 20 N-m Load (max. nominal load) on PR70 Powercube (two identical point plots; near perfect overlap is due to the precision of the position controller)

6.1.1.2. Drill Components

The drill used in the tines and no-tines experiments is shown in Figure 8. It is a COTS rotary/percussive drill made by Bosch and has the following specifications:

- 24V, 15 amps (in percussive mode during nominal coring)
- 1200 RPM, 4400 BPM (beats per minute in percussive mode)
- ~2kg (without battery)
- 1.4 J impact energy

Figure 8: External and Internal Views of the Bosch Hammerdrill

The coring bit used was also a COTS part made by Relton with the following specifications:

- High speed steel with brazed carbide tips
- 1 cm inner diameter
- Maximum coring depth ~4cm
- 3/8" centering bit

Figure 9: New Coring Bit with Centering Bit (left) and Worn Coring Bit without Centering Bit (right)

The drill current sensor used was also a COTS part. This Hall effect sensor measured the total current being provided to the drill. The signal was read using the A/D board described below in Avionics.

6.1.1.3. Force/Torque Sensor

The force/torque sensor (see Figure 10) used was a COTS part made by ATI Industrial Automation. This sensor measured three orthogonal forces and three orthogonal torques. Table 2 shows the specifications of the sensor used, the Gamma SI-130-10. This sensor was used in the tines experiments to measure the preload. In the no-tines experiments it was used to measure the coring force.

Figure 10: ATI Force/Torque Sensor

Specification	Gamma SI-130-10
F_x, F_y range (+/- N)	130
F_z range (+/- N)	400
T_x, T_y, T_z range (+/- N-m)	10
F_x, F_y resolution (N)	1/160
F_z resolution (N)	1/80
T_x, T_y, T_z resolution (N-m)	1/3200
F_{xy} overload (+/- N)	1200
F_z overload (+/- N)	4100
K_x, K_y stiffness (N/m)	9.1×10^6
K_z stiffness (N/m)	18×10^6
K_{tx}, K_{ty} stiffness (N-m/rad)	11×10^3
K_{tz} stiffness (N-m/rad)	16×10^3
Sensor mass (kg)	0.250
Diameter (m)	0.0754
Height (m)	0.0333

Table 2: Specifications of the Force/Torque Sensor Made by ATI Industrial Automation

6.1.1.4. Avionics

The avionics needed to operate the arms consisted of the following items:

- Linux computer (1 GHz Intel PIII SMP) running 2.4 kernel
  - CANbus card for communication (ESD-PCI/331)
  - A/D card for F/T and drill current sensors (NI-6036e)
- 24V and 48V power supplies
- ATI F/T sensor conditioning box

6.1.1.5. Configuration

The configuration of both arms used during the tines and no-tines experiments were very similar. They both had the same first 5 joints connected in the same kinematic configuration (see Figure 11). The joints were arranged as yaw/pitch/pitch/pitch/yaw (YPPPY) using the three different sizes PR110, PR110, PR90, PR70, and PR70 respectively. Switching between the two configurations (they actually used the same hardware) took minimal effort and time.

Figure 11: No-tines Arm Configuration (left) and Tines Arm Configuration (right)

6.1.2 No-Tines Specific

There was no hardware that was specific to the no-tines coring experiments. However, the configuration of the arm was slightly different. The no-tines configuration used 2 links of equal length (0.75 cm). The F/T sensor was mounted to the 5th joint, between the joint and the drill. The drill was mounted to the F/T sensor using compliant mounts designed to protect the F/T sensor from the impact forces generated by the percussive drill. In this configuration a Cartesian motion of the arm provided the linear coring motion.

6.1.3 Tines Specific

Hardware that was specific to the tines coring experiments included the tines plate (Figure 12) and the linear stage (Figure 13). The tines plate consisted of a single piece of machined aluminum that attached directly to the bottom of the linear stage. Threaded into the aluminum were three tines made of high strength sharpened fasteners. The linear stage was a ball screw mechanism with the same motor and interface as the PR70 joints (see Table 3).

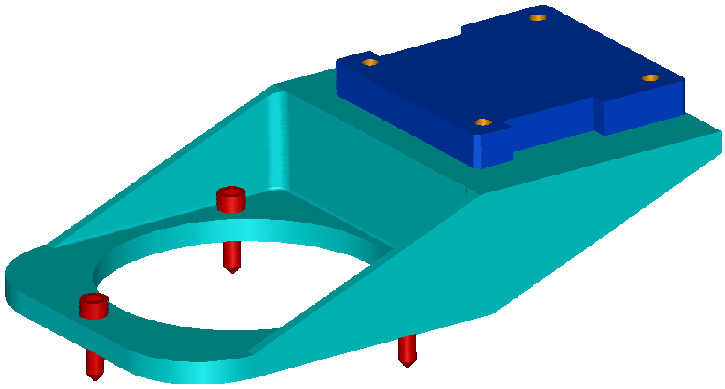

Figure 12: Tines Plate

Figure 13: Amtec Linear Stage

Specification	**LS70**
Drive Force (N)	600
Resolution (ticks/mm)	33333
Max. Velocity (mm/sec)	4.0
Repeatability (+/- mm)	0.01
Power (W)	125
Mass (kg)	4.5

Table 3: Specifications of the Linear Stage Made by Amtec-Robotics

The configuration of the arm during the tines experiments was different because the second link was significantly shorter, 0.32 meters, than the no-tines configuration. The reason for the shorter link was because of torque limitations of the elbow joint due to the extra mass from the linear stage.

The linear stage was mounted to the F/T sensor using compliant mounts, again, to isolate the F/T sensor from the impact forces generated by the percussive drill. The drill was then mounted directly to the linear stage. In this configuration the linear stage provided the linear coring motion.

6.2. Software

6.2.1 Common

Most of the software was common between the tines and the no-tines experiments. At the driver level, several vendor based software products were used:

- A/D card driver (Comedi open source project)
- CANbus driver (ESD vendor product)
- Powercube (motor) driver (Amtec product)

The A/D card drive was provided by an open source project called Comedi. It was a kernel module that provided a C library interface to the National Instruments A/D card and all of its functionality.

The CANbus driver was a kernel module that provided a C library interface to the communication layer of the CANbus card. This interface received bus commands and broadcast them over the serial bus.

The Powercube driver was a product that was provided from Amtec-Robotics (the same company that made the joints). This driver was a C++ library that provided access to the entire command set available for the joints. It used the CANbus driver to broadcast these commands over the bus. The command set included command and telemetry functions such as: get joint position, get joint velocity, get joint acceleration, set joint position, set joint velocity, set joint acceleration, etc. Full a full command set see [7].

Above the driver level, the CLARAty software architecture was used. Several modules were developed to enable the task level operation of the tines and no-tines arms. The modules that were common to tines and no-tines experiments include:

- Motor interface
- F/T sensor interface
- Forward/inverse kinematics
- Trajectory generation

The interface to both the tines and no-tines was virtually identical. The commands were desired tool pose. It had to be manually determined where the target was and what its normal vector was. The telemetry included the 5 DOF pose of the tool, the force/torque measurements, the drill speed and current, and the joint angles.

The task level algorithms for coring were different for the tines and no-tines experiments and are discussed below.

6.2.2 No-Tines Specific

The general task level algorithm for no-tines coring is described Section 4.2.1. The single-axis force control method was used in the experiments discussed here. The only difference between the algorithm described and the algorithm implemented was that the target location and normal were calculated manually rather than from stereo imagery. After the arm moved to the initial pose commanded by the user (which was assumed to be offset from the target by a nominal distance, ~ 1 cm), the coring algorithm began. The algorithm then started a z-axis tool move with the rate of the move being proportional to the error between the nominal coring force and the measured coring force. The measured coring force was a heavily filtered value based on the z-axis force of the force/torque sensor (see Figure 14). The tool move is a Cartesian motion calculated with the inverse kinematics and the trajectory generation modules described above. The nominal stop condition for coring was when a predefined coring depth had been reached.

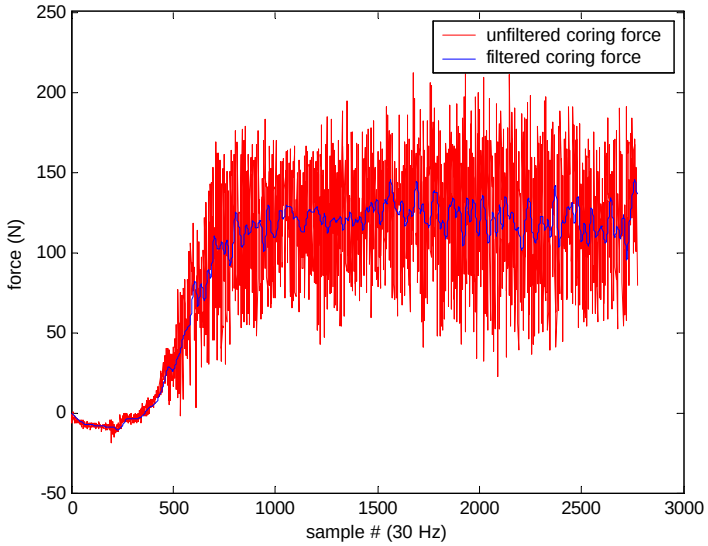

Figure 14: Illustration of Force Filter Used for Coring Force Measurement

6.2.3 Tines Specific

The general task level algorithm for tines coring is described Section 4.1.3. This section discusses the actual algorithm implemented for the tines experiments. This task level algorithm consisted of two separate, but similar, algorithms: one for applying a preload, and the other for coring.

The preload algorithm for the no-tines experiment was identical to the coring algorithm for the tines experiment. The only difference was that the nominal stop condition for the preload algorithm was a short time (1-2 seconds) after the force setpoint had been met rather than when a coring depth had been reached. The preload setpoint was normally set to be 130 N, which was approximately 10 N above the known coring force setpoint. This prevented the tines from 'walking' during the coring process. In a flight system, a larger margin would certainly be used.

The tines coring technique was different from the no-tines coring technique in two ways: the feedback sensor was different and the mechanism that provided the linear coring motion was different. The feedback sensor for the tines experiments was different because of the fact that the coring force became unobservable by the F/T sensor after the preload had been applied. Therefore, the drill current sensor had to be used to control the coring feedrate. An approximately linear relationship existed between the drill current and the coring force (see Figure 15). The second difference, the linear stage, was simply a different mechanism to provide the linear motion required for coring. Even though a different feedback sensor was being used and a different mechanism for providing the coring feedrate, the exact same algorithm as the no-tines coring (with different parameter values) was used to determine the coring feedrate.

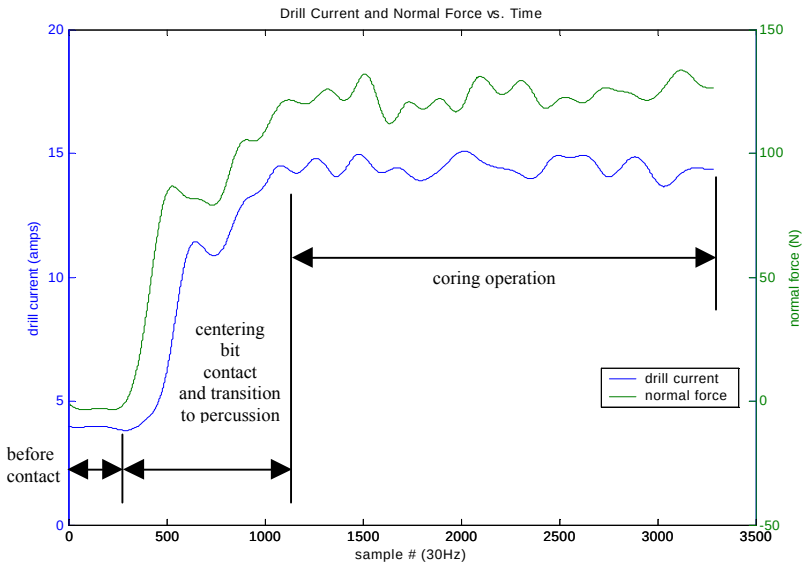

Figure 15: Drill Current and Normal Force vs. Time during a Coring Experiment

6.3. Rocks

Several types of rocks were used during the experiments. A summary of these rocks and their mechanical properties are shown in Table 4.

Rock Type	Typical Compressive Strength (Mpa)
Granite	175
Quartzite	225
Concrete	40
Basalt	200

Table 4: Typical Compressive Strength of Cored Rocks

7. Experimental Results

Many cores were drilled in the course of the tines and no-tines experiments. A total of approximately 1 meter of coring depth was performed through various types of rocks over about 6 months of testing. There were several main goals (listed in order of importance):

- To determine if intact cores could be taken with both the tines and no-tines methods
- To compare the effectiveness of the tines and no-tines methods
- To compare the complexity (algorithmic and electro-mechanical) of the tines and no-tines methods
- To determine if drill current could be used to control coring feedrate
- To compare closed-loop and open-loop coring methods
- To confirm the utility of a centering bit

The most significant result from the tines and no-tines experiments was the demonstration that achieving an intact core was possible using both the tines and no-tines techniques. Figure 16 is an example of one of the intact cores taken.

In order to achieve an intact core, a coring bit without a centering bit had to be used (see Figure 9). The reason for this requirement was because the relative size of the outer diameter of the centering bit and the inner diameter of the coring bit left only a few millimeters of material (not enough to stay together as an intact core). The result of not using a centering bit (for both the tines and no-tines cases) was that the coring hole had to be started manually (using a drill press) to a depth of approximately 1 mm. Then, during the experiments, just before the coring bit touched the rock, the bit had to be guided by hand into the previously started hole. Also, as may be expected, this method successfully achieved intact cores in only a few types of rock, namely the basalt and granite. The significance of this anecdote is twofold: first, a centering bit is very good at enabling a coring system (even with low stiffness) to start coring, and second, if a centering bit is not to be used, the stiffness between the tool and the environment must be extremely stiff (like a drill press).

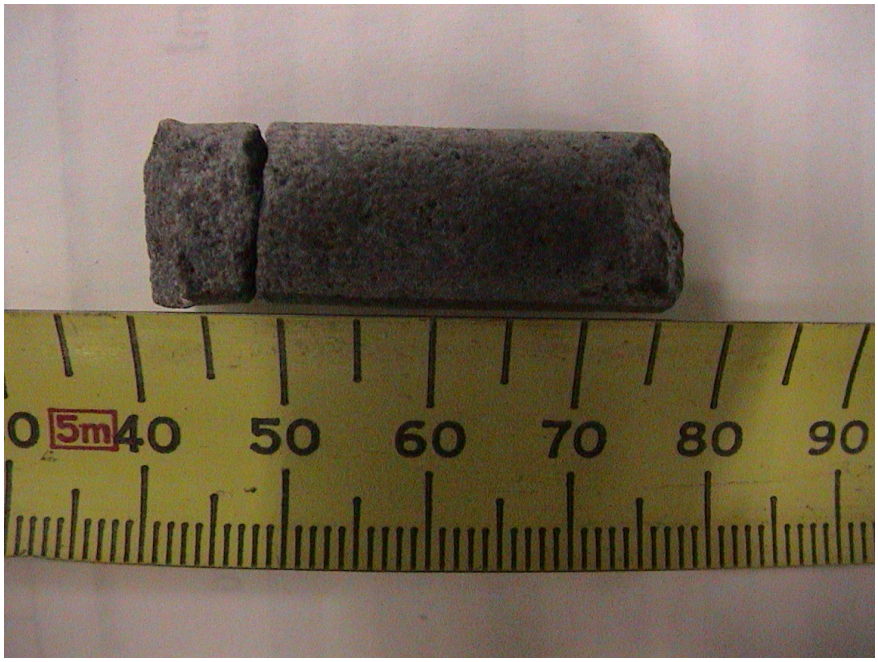

Figure 16: Intact Core Taken with No-tines Technique in Granite

7.1. No-tines

Many no-tines experiments were performed during the course of this task. This section shows typical results from these experiments. These experiments were performed using the rocks shown in Table 4. It is beyond the scope of this document and this task to characterize the differences between coring these rocks, except for the fact that the coring rate (resulting from feedback control) was significantly correlated to the rock compressive strength (the stronger the rock, the lower the coring rate). Figure 17 shows that without using some kind of force feedback (including current feedback) it was difficult to core into a rock of unknown properties. With a constant coring velocity, the coring force exponentially increased with depth and eventually the experiment was aborted. If a small enough velocity were commanded this would not happen, however this velocity would have to be low enough to core through the hardest rock expected.

Figure 18 shows data from a typical no-tines experiment using basalt. The blue line is a filtered coring force measurement and the red line is the commanded depth. The coring force setpoint in this experiment was 120 N. As can be seen, this setpoint is followed reasonably well, with an 8.8 N RMS error (after setpoint was initially reached at ~50 sec). The average coring rate in this experiment was ~1.8 cm/min. It is important to note that approximately the first 6 cm of depth shown in the plot is not actually coring bit penetration depth, but is due to the initial approach distance to the rock (~1.0 cm), the length of the centering bit before the coring bit (~2.5 cm), and the deflection of the arm (~2.5 cm). The actual coring depth reached in this experiment was approximately 4.5cm.

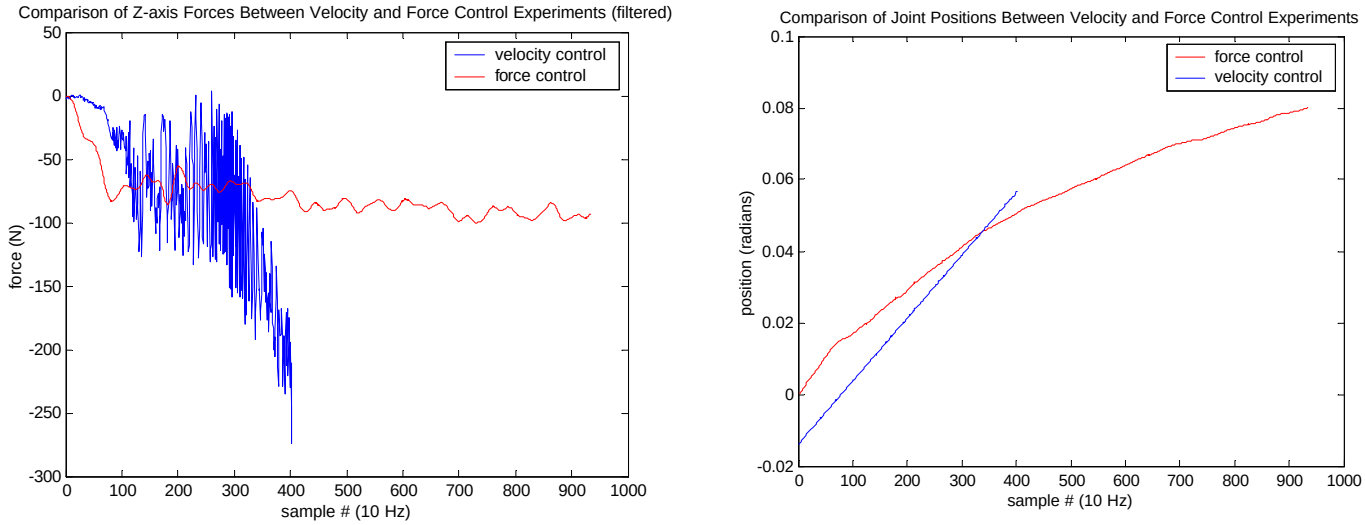

Figure 17: Plots Demonstrating the Difficulty of Coring without Force Feedback

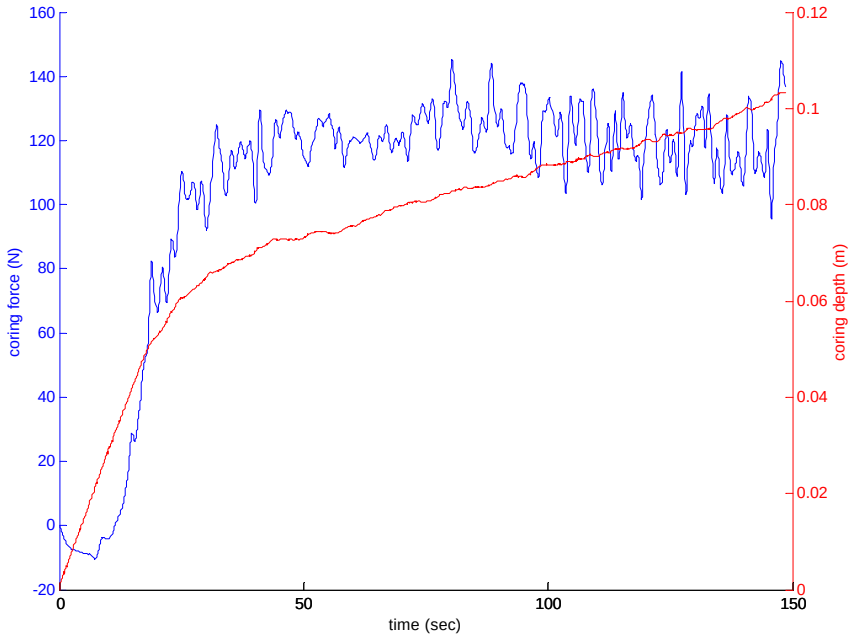

Figure 18: Coring Depth and Coring Force vs. Time for No-tines Experiment

7.2. Tines

Many tines experiments were performed during the course of this task. This section shows typical results from these experiments. These experiments were performed using the rocks shown in Table 4.

Figure 19 shows the drill current and coring depth for a typical tines experiment in concrete. Drill current was used as the feedback variable in the tines experiments. As can be seen in Figure 19, the drill current goes through three distinct phases. The first phase (at ~2 amps) is before the bit touches the rock. The second phase (at ~5 amps) is after the bit touches the rock but before the percussive action of the drill begins. The third phase (at ~14 amps) is after the percussive action of the drill begins. The current setpoint used for this experiment was 15 amps. Similar to Figure 18, the depth shown in the plot is not the actual penetration depth of the coring bit. For the same reasons discussed above, the actual penetration depth was ~3.1 cm. The average coring rate during this experiment was ~2.9 cm/min. Figure 20 shows the z-axis force measurement by the wrist force/torque sensor. This sensor was behind the tines, so theoretically, if the coring forces never exceeded the preload force, then this measurement should remain at a constant value equal to the preload force (130 N), throughout the coring process. This is obviously not the case. Approximately 30 seconds into the experiment, the percussive action of the drill began. As can be seen, the force measurement exceeds 130 N several times. During these periods the potential for tines walking existed, however, no significant walking was observed. It is also noticeable that the average force measured during the coring experiment seems to be significantly smaller than 130 N. There are several possible explanations for this. First, the tines did sink further into the surface of the rock during the coring process; this would reduce the preload seen by the force sensor. Another possibility would be that the joints in the arm were backdriven during the coring process; the brakes were enabled during the coring experiment, but it is possible that they were backdriven (the holding torque of the brake is not known) under such high vibrational loads.

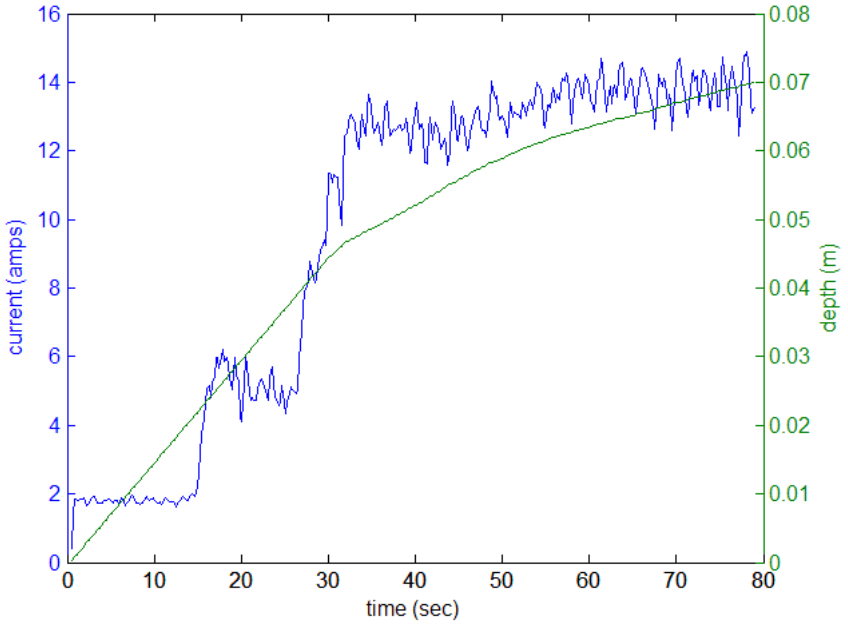

Figure 19: Coring Depth and Drill Current vs. Time for Tines Coring Experiment

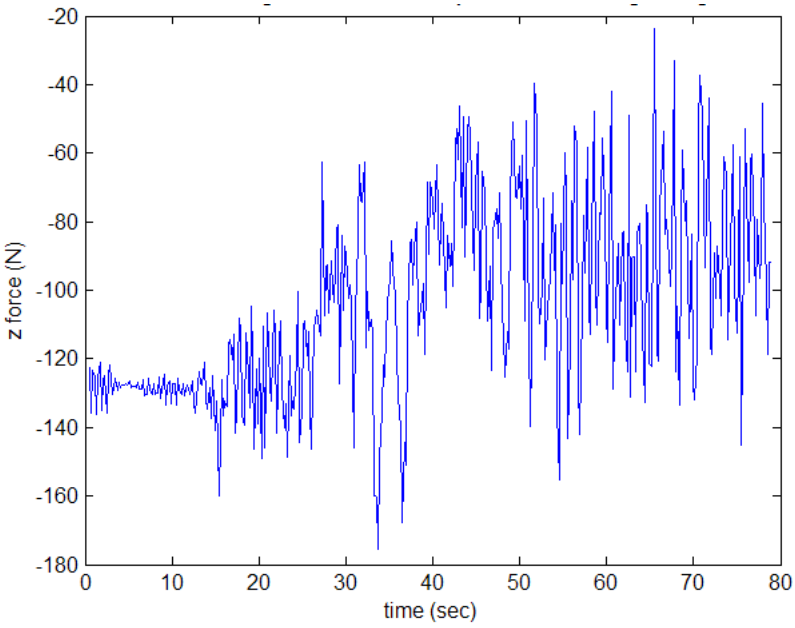

Figure 20: Filtered Z Force as Seen by F/T Sensor During Coring

8. Summary

This document is meant to contribute data and conclusions for the tines/no-tines decision that will have to be made by the flight SA/SPaH team. It is hoped that it adds to the discussion by bringing up issues that may not have been thought of, by demonstrating quantitative results from relevant experiments, and by drawing important conclusions based on experiments. One of the major conclusions of this study has been that it is possible to take intact cores with both the tines and the no-tines methods. This important fact was unclear before the experiments were performed.

The comparison criteria discussed in Section 5 is by no means an exhaustive list of all possible comparison criteria, but it is believed that these are the most significant criteria that will affect the decision between tines and no-tines.

The experimental setup was designed to be a representative system that could be analyzed and referenced. The hardware design was very similar to the current baseline design, in terms of the distributed nature of its motor control, and its use of brushless motors, electro-magnetic brakes, and harmonic drives. The software design allowed rough comparisons of algorithm complexity between the tines and no-tines techniques, resulting in the conclusion that there would not be significantly different levels of complexity between the techniques.

At the highest of levels it was not determined whether one technique was superior to the other. A more sophisticated systems-level trade, beyond the scope of this task, must be done to draw any significant conclusions. It is hoped, that this work will contribute to that trade.

9. References

[1] Mars Technology Development Program Corer/Abrader Tool Brassboard Technology Announcement (July 23, 2004).

[2] Design documents from the MSL Actuators, Lubricants, & Bearings task (managed by Mike Johnson).

[3] Eric T. Baumgartner, Robert G. Bonitz, Joseph P. Melko, Lori R. Shiraishi and P. Chris Leger, "The Mars Exploration Rover Instrument Positioning System", Proceedings of the IEEE Aerospace Conference, March 2005.

[4] Conversations with Bob Bonitz.

[5] S. P. Gorevan, et al., "Rock Abrasion Tool: Mars Exploration Rover Mission," Journal of Geophysical Research, 108(E12), 8068, doi:10.1029/2003JE00 2061, 2003.

[6] D. Helmick, A. Okon, "Force Sensing Comparison Report," JPL Technical Report, June, 2005.

[7] Amtec-Robotics, "Programmers Guide for PowerCube," Version 1.2, July 30, 2004.